Journal of the European Ceramic Society 23 (2003) 437–443

www.elsevier.com/locate/jeurceramsoc

Morphology and microstructure in the sintering of β-spodumene precursor powders with TiO_2 additive

Moo-Chin Wang[a,*], Nan-Chung Wu[b], Sheng Yang[b], Shaw-Bing Wen[c]

[a]*Department of Mechanical Engineering, National Kaohsiung University of Applied Sciences, 415 Chien-Kung Road, Kaohsiung, 80782, Taiwan*
[b]*Department of Materials Science and Engineering, National Cheng - Kung University, 1 Ta-Hsueh Road, Tainan, 70101, Taiwan*
[c]*Department of Resources, National Cheng -Kung University, 1 Ta-Hsueh Road, Tainan, 70101, Taiwan*

Received 25 July 2001; received in revised form 27 March 2002; accepted 11 April 2002

Abstract

The effect of TiO_2 additions on the morphology and mechanism of sintering β-spodumene ($Li_2O{\cdot}Al_2O_3{\cdot}4SiO_2$, LAS_4) glass-ceramics using organometallic precursor powders was investigated by X-ray diffractometry (XRD), scanning electron microscopy (SEM), transmission electron microscopy (TEM) and electron diffraction (ED). The crystalline phase formation in the calcination of LAS_4 precursor powders added with TiO_2 has shown a major phase of β-spodumene and a minor phase of rutile. The fraction and size of pores decrease rapidly with sintering temperature increasing from 950 to 1350 °C. The pores were mainly interconnected at the sintering temperatures $\leqslant$ 1050 °C; and become completely isolated at the sintering temperature of 1250 °C. The rutile precipitated in sintering of β-spodumene glass-ceramics prepared from LAS_4 precursor powders with TiO_2, appears in two different forms: the one with the size of about l.0 μm mainly segregates and agglomerates at the grain boundaries of β-spodumene; and the other consists of a few precipitates dispersed within the β-spodumene grains.

Keywords: Glass ceramics; Microstructure; TiO_2; Precursors; Sintering; β-Spodumene; Rutile

1. Introduction

Low thermal expansion glass-ceramics have several applications where the dimensional stability and/or ability to resist thermal shock are necessary. Li_2O–Al_2O_3–SiO_2 glasses are known as base glasses for low thermal expansion glass-ceramics and many experiments have been conducted on phase equilibria[1–3] and crystallization[4–11] in this system.

β-Spodumene ($Li_2O{\cdot}Al_2O_3{\cdot}4SiO_2$, LAS_4) has a tetragonal dipyramid crystal structure[12] which is uniaxial positive.[3] Li and Peacor[13] pointed out that the structure of β-spodumene consists of a 3-dimensional network of Si–O and Al–O tetrahedra. These tetrahedra are randomly distributed in the network; with the Li ions in the interstitial positions.

Conventionally, glass-ceramics have been fabricated by usual glass forming techniques, e.g. blowing, pressing, or casting, followed by nucleation and crystallization. Glass-ceramics also can be produced by sintering and crystallization of glass powders. This permits the reduction of processing temperature and the fabrication of complex shapes using a variety of ceramic formation techniques, e.g. dry pressing, slip casting, tape casting, extrusion, and injection molding.[12]

Most crystallizable glass powders are difficult to sinter because of the large surface area for nucleation, promoting crystallization from the surface of every glass particle toward the center and inhibiting effective sintering to achieve full density.[14] Although several workers attempted to sinter β-spodumene glass-ceramics by using spodumene composition glass powders,[15,16] it has been shown that stoichiometric spodumene glass does not sinter well. Adding a small amount of B_2O_3 and/or P_2O_5 was found to be necessary to control the sintering/crystallization behavior of the β-spodumene glass-ceramics. It is well known that it is not easy to sinter β-spodumene glass-ceramics without proper sintering aid agents, unless the alkoxide-derived precursors are used.[17–19] The incorporation of sintering aid agent can result in a large thermal expansion increase. Therefore, the preparation of homogeneous fine β-spodumene powders has been considered to be indispensable.

* Corresponding author.
E-mail address: dragon@cc.kaus.edu.tw (M.-C. Wang).

0955-2219/02/$ - see front matter
PII: S0955-2219(02)00095-X

In the present study, the spodumene ($Li_2O{\cdot}Al_2O_3{\cdot}4SiO_2$,LAS) precursor powder with a chemical composition of Li^{9+}, Al^{3+} and Si^{4+} ions in a stoichiometric molar ratio of 1:1:2 was prepared by sol-gel processing. The TiO_2 powders were prepared by a wet method using $Ti(OC_2H_5)_4$ as a starting material. The effect of TiO_2 addition on the morphology and mechanism for sintering of β-spodumene glass-ceramics was examined by differential thermal analysis (DTA), X-ray diffractiometry (XRD) analysis, scanning electron microscopy (SEM), transmission electron microscopy (TEM), and electron diffraction (ED) analysis.

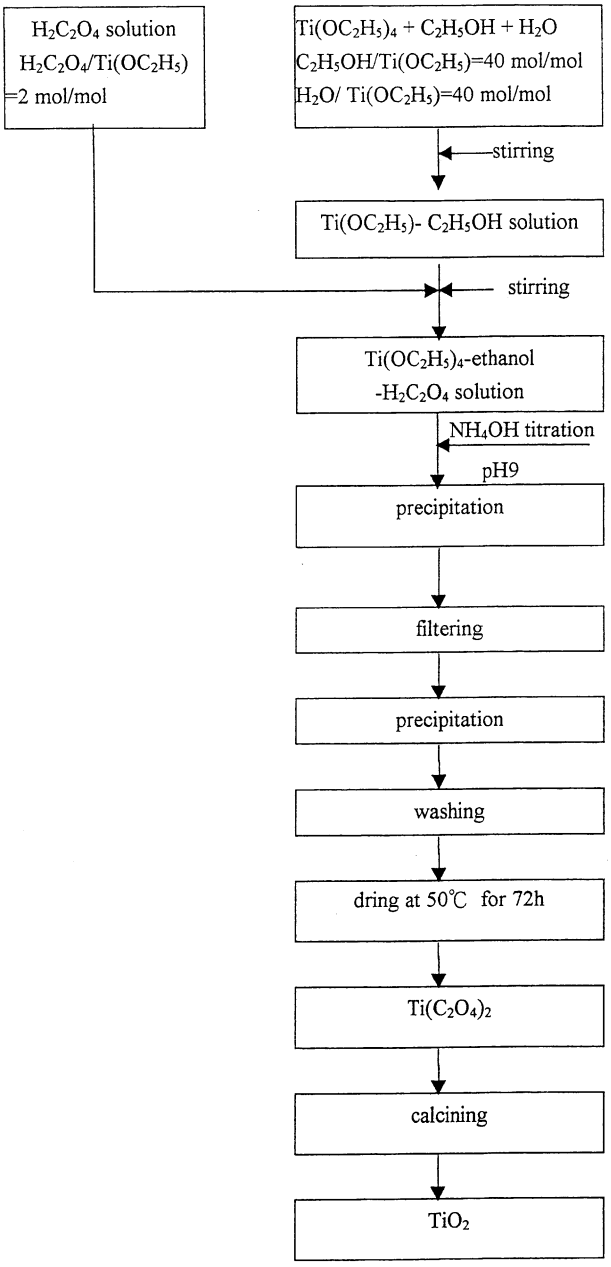

Fig. 1. Schematic diagram of the wet-method for preparing TiO_2 powders using $Ti(OC_2H_5)_4$ as a starting materials.

The purposes of this investigation are to (i) demonstrate the effect of TiO_2 addition on the crystallization of β-spodumene in the LAS_4 precursor powders, (ii) observe the morphology of sintered LAS_4 precursor powders with TiO_2 additive, and (iii) observe the microstructure in the sintering of β-spodumene precursor powders containing TiO_2.

2. Experimental procedure

2.1. Sample preparation

The precursor powders with a spodumene composition ($Li_2O{\cdot}Al_2O_3{\cdot}4SiO_2$,$LAS_4$) were prepared from tetraethylorthosilicate [$Si(OC_2H_5)_4$, TEOS], aluminum trisecbutoxide [$Al(OC_4H_9)_3$, ASB] and lithium nitrate ($LiNO_3$) as the starting materials. The TEOS, ASB and $LiNO_3$ were supplied by Janssen Chemical Co. (Belgium), Aldrich Co. (USA) and Fluka Co. (Switzerland), respectively. The preparation process of the spodumene precursor was described in detail in our previous report.[20,21]

The TiO_2 powders were prepared from Ti-ethoxide ($Ti(OC_2H_5)_4$) as a starting material. $Ti(OC_2H_5)_4$ was supplied by Ferak Co.(Germany). The schematic flowchart of the TiO_2 powders preparation by a precipitation process is shown in Fig 1.

The LAS_4 precursor powders containing 5.0 wt.% TiO_2, were prepared from the calcined LAS_4 precursor powders. The mixture was blended for 4 h in a laboratory ball mill containing aluminum oxide balls and ethanol. Pellets were prepared from 0.45 g dried powder mixtures by uniaxial pressing at 176 MPa in a stainless

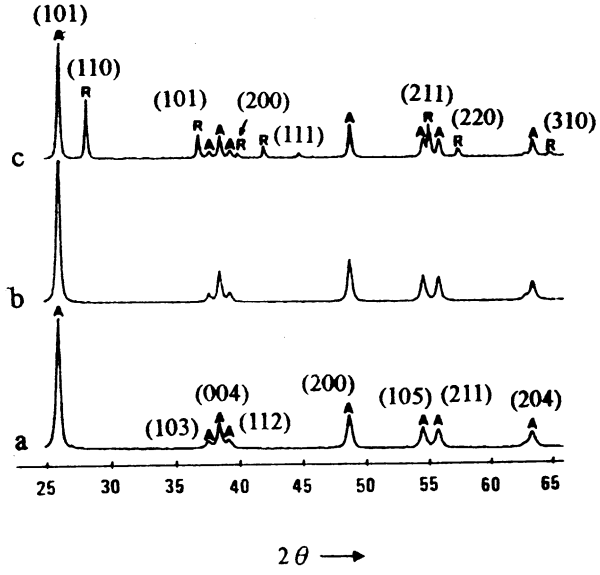

Fig. 2. XRD patterns of $Ti(C_2O_4)_2$ calcined at various temperatures for 4 h: (a) 450 °C, (b) 550 °C, and (c) 650 °C. A: anatase-type TiO_2 ; R: rutile-type TiO_2.

steel die with a diameter 30.0 mm. The pellets were sintered in air at a heating rate of 4 °C·min^{-1} to 950–1350 °C and held 5–10 h.

2.2. Characterization

The crystalline phase was identified by an XRD analysis. The XRD was done with a Rigaku X-ray diffractometer with CuK_α radiation and a Ni filter, at a scanning rate of 0.25°C·min^{-1}. The samples were prepared by crushing the sintered bodies and passing the powder through a −325 mesh sieve. A Jeol JSM-840 scanning electron microscopy was used to examine the surface morphology of polished, fractured, and etched (5 parts HF, 2 parts HCl and 93 parts H_2O) samples coated with a thin gold film.

The transmission electron microscopic (TEM) epamination was carried out using a JEM 200 microscope operated at 200 kV. Electron diffraction (ED) pattern was made on thinned foil specimens of the sintered samples. The 3 mm diameter TEM disks were cut from the bulk with an ultrasonic cutter and mechanically thinned by hand to a thickness of 80 μm or less using diamond paste. The final thinning was done by ion-milling to electron transparency.

3. Results and discussion

3.1. Phase evolution of $Ti(C_2O_4)_2$

The X-ray diffraction (XRD) patterns of the dried precipitates of $Ti(C_2O_4)_2$ calcined at various temperatures for 4 h are shown in Fig. 2. The effect of calcination on the evolution of different crystalline forms of titanium dioxide is as follows: (a) at 400 °C; the anatase-type titanium dioxide is precipitated, and the major reflection

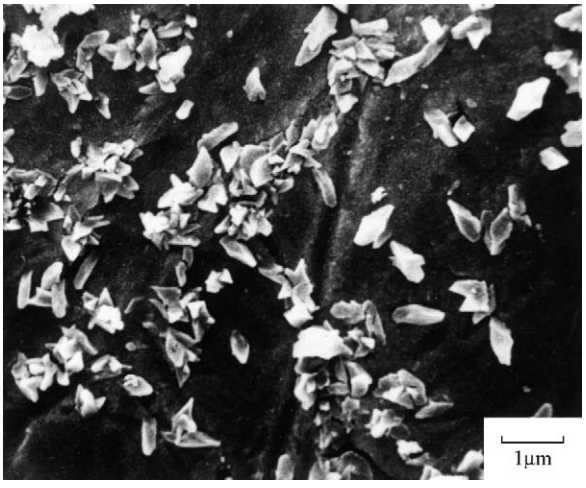

Fig. 3. Typical SEM micrograph of the precipitates of $Ti(C_2O_4)_2$ after drying at 50 °C for 72 h.

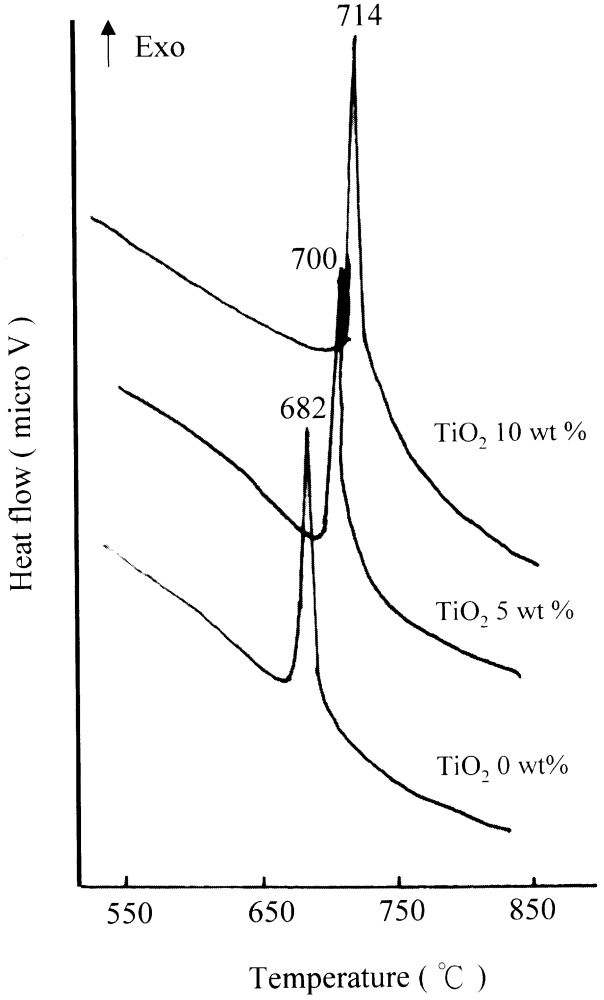

Fig. 4. DTA curves for LAS precursor powders with 0, 5 and 10 wt.% TiO_2 at a heating rate of 10^4°C·min^{-1} respectively. (a) 0 wt.% (b) 5.0 wt.% and (c) 10.0 wt.%.

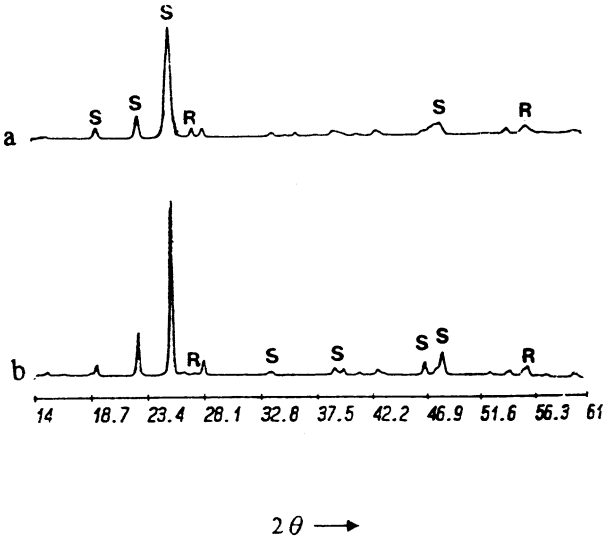

Fig. 5. XRD patterns of the LAS_4 precursor powders containing 5.0 wt.% TiO_2 as sintered at various temperatures for 5 h: (a) 950 °C and (b) 1350 °C. S: β-spodumene, R: rutile.

corresponds to (101), (103), (004), (112), (200), (105), (211) and (204) of the anatase-type TiO_2; (b) at 500 °C, the crystallized phases maintain the anatase–type TiO_2, and (c) at 700 °C, the XRD patterns are representative of the anatase and rutile type crystals. No other phases are found. The crystallinity of the rutile phase is improved by increasing calcination temperature from 600 to 700 °C.

Fig. 3 shows the SEM micrograph of the morphology and particle size of the dried precipitates of $Ti(C_2O_4)_2$ from $Ti(OC_2H_5)_4$–ethanol–$H_2C_2O_4$ solution. The particles of $Ti(C_2O_4)_2$ from this solution are of the polygonal shape. The particle of $Ti(C_2O_4)_2$ has the largest edge of 0.6 μm, and the lowest edge of 0.1 μm.

3.2. -Phase evolution of the LAS_4 powder with TiO_2 additive-

The DTA curves for the samples at a same heating rate of 10 °C·min^{-1} were shown in Fig. 4. On heating the LAS_4 precursor with no TiO_2 [Fig. 4(a)], a sharp exothermic reaction peak at 682 °C was due to the formation of β-spodumene.[20] For the LAS_4 precursor powders with 5.0 and 10.0 wt.% TiO_2, the exothermic peaks of β-spodumene phase formation were at 700 and 714 °C, respectively. It can be seen that the exothermic reaction temperature of LAS_4 precursors containing TiO_2 powders was higher than that without TiO_2 addi-

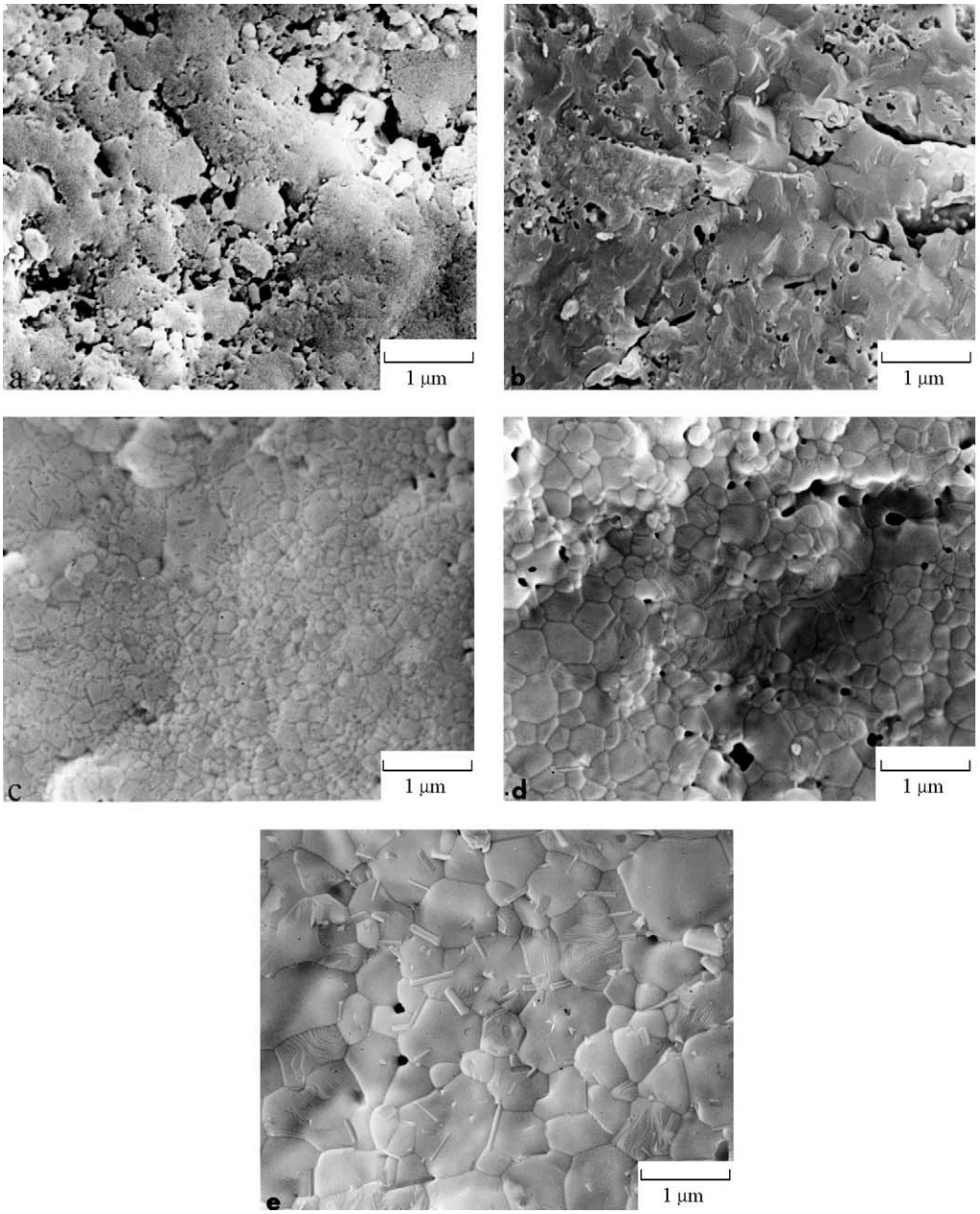

Fig. 6. SEM surface morphology of the LAS_4 precursor powders containing 5.0 wt.% TiO_2 as sintered at different temperatures for 10 h: (a) 950 °C, (b) 1050 °C, (c) 1150 °C, (d) 1250 °C and (e) 1350 °C.

tion, and the exothermic peak shifts to a higher temperature with increasing TiO_2. This phenomenon is opposite to the result of Barry et al.[22]

Fig. 5 shows the XRD patterns of the sintered bodies for the uncalcined Li_2O–Al_2O_3–$4SiO_2$(LAS_4) powders added with 5.0 wt.% TiO_2 and sintered at 950 and 1350 °C for 5 h, respectively. The compact body sintered at 950 °C for 4 h only has the sharp peaks corresponding to the crystalline phase of the β-spodumene and a small amount of rutile TiO_2 are observed. No broad scattering spectrum indicates that the crystallization process of the amorphous LAS_4 precursor powders approaches completion. As the compact body is sintered at 1350 °C for 5 h, the β-spodumene phase is apparently promoted at higher temperatures, and a minor crystalline, rutile TiO_2, also appears. The above behavior of the phase evaluation in the present process is the same as that of the gel-derived Li_2O–Al_2O_3–$4SiO_2$–$n TiO_2$ powders.[23–25]

3.3. Morphology of sintered bodies

According to the XRD analysis, the LAS_4 precursor powders added with TiO_2 and sintered at 950 °C contain mainly β-spodumene and a small amount of rutile.

The surface morphology of the LAS_4 precursor compacts containing 5.0 wt.% TiO_2 and sintered at different temperatures for 10 h was shown in Fig. 6. By reducing the sintering at 950 °C for 10 h, TiO_2 addition can produce β-spodumene glass-ceramics with a little particle coalescence [Fig. 6(a) and (b)]. The largest voids were much greater than that obtained at other sintering temperatures. The fraction and size of the pores decrease rapidly with increasing temperature from 950 to 1350 °C. Fig. 6 indicates that the pores were mainly interconnected at 950–1050 °C, and become isolated as the sintering temperature was increased to 1250 °C. The grain structure in Fig. 6(a) was not well-defined. However, the well-defined grain structure can be seen for the samples sintered at higher temperatures [Fig. 6(d) and (e)]. The grain size of the samples sintered at 1350 °C was much greater than that at 1050 °C.

On the surface of the sintered bodies as shown in Fig. 6, no rutile was formed at the sintering temperature ranging from 950 to 1150 °C. As the sintering temperature is raised to 1250 °C, the rutile with needle morphology is initially precipitated on the surface of the sintered bodies. The needle rutile precipitates with increasing sintering temperature.

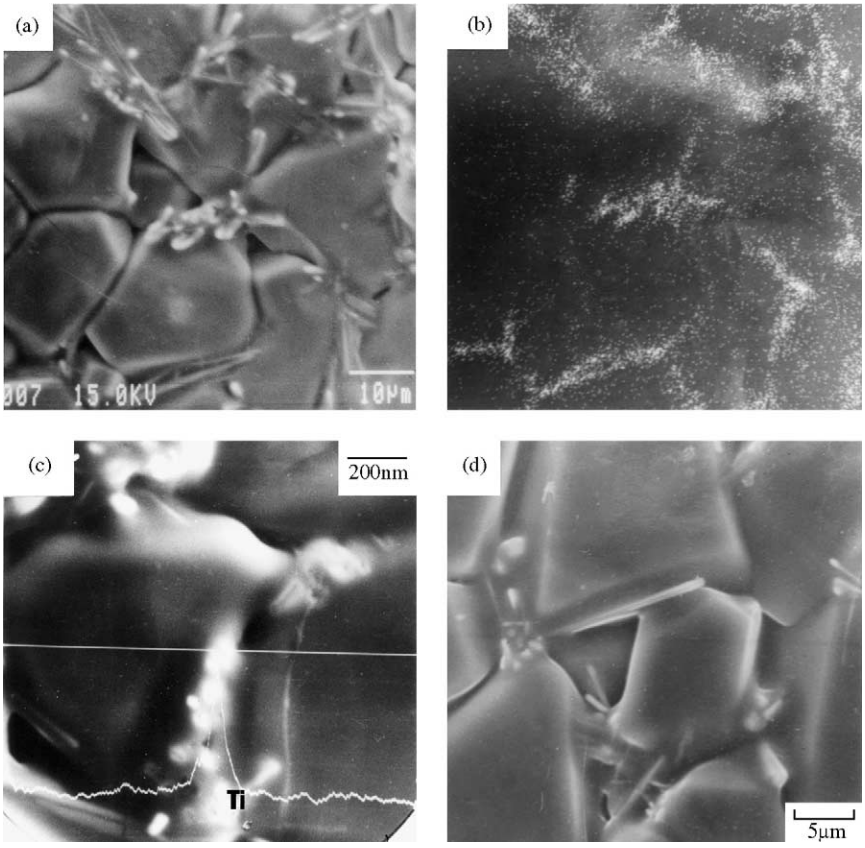

Fig. 7. The polished microstructure of the LAS_4 precursor powders added with 5.0 wt.% TiO_2 and sintered at 1350 °C for 5 h. (a) The rutile precipitated and segregated at the grain boundaries of the β-spodumene grains and a few tiny precipitated dispersed within the β-spodumene grains; (b) the image scanning of Fig. 7(a) for Ti element; (c) the line scanning of Ti element; (d) the rutile at the β-spodumene grain boundaries with a liquid base.

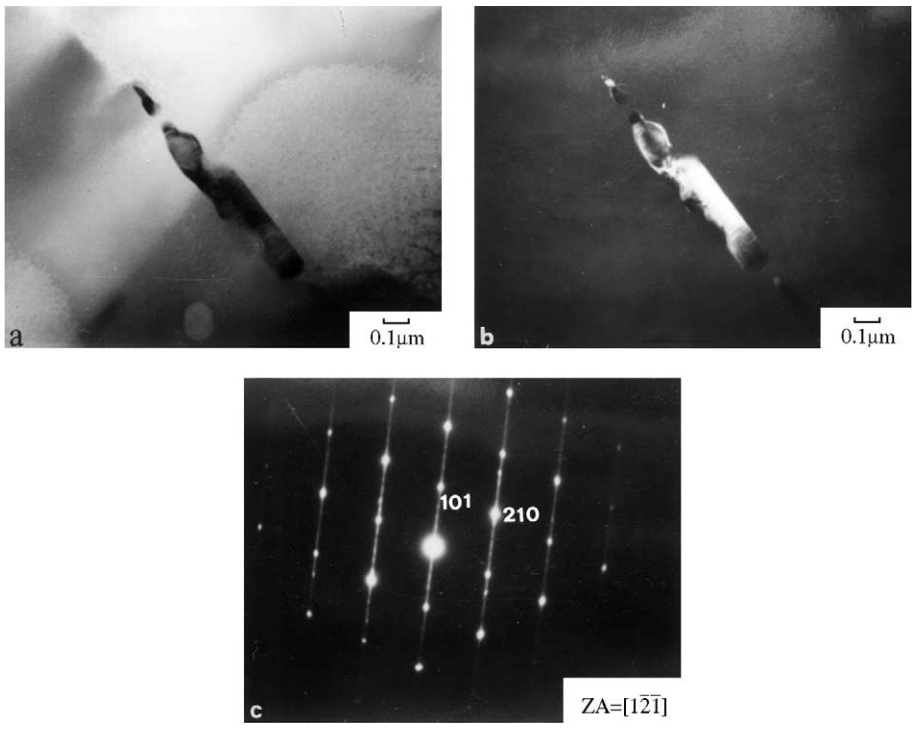

Fig. 8. TEM micrograph of the LAS_4 precursor powders contianing 5.0 wt.% TiO_2 as sintered at 1350 °C for 5 h: (a) bright field image; (b) dark field image; (c) electron diffraction pattern corresponding to the rutile phase

3.4. Microstructure of sintered bodies

The polished microstructure of the LAS_4 precursor powders added with 5.0 wt.% TiO_2 content and sintered at 1350 °C for 5 h was shown in Fig. 7. Fig. 7(a), shows that rutile precipitated in this sintered sample appears in two different forms. The larger precipitates, about 1 μm, were segregated and agglomerated at the grain boundaries of the β-spodumene crystalline grains. A few precipitates were dispersed within the β-spodumene crystalline grains. The image scanning analysis of Fig. 7(a) for titanium was shown in Fig. 7(b). The result also indicates that titanium was mainly segregated at the grain boundaries. The line scanning analysis of titanium was shown in Fig. 7(c). Most of titanium are trapped in the grain boundaries of the β-spodumene crystalline grains. The rutile resides mostly at the β-spodumene grain boundaries with a residue of a formerly liquid phase as shown in Fig. 7(d).

The TEM micrograph of the LAS_4 precursor powders added with 5.0 wt.% TiO_2 and sintered at 1350 °C for 5 h is shown in Fig. 8. The larger crystalline phase is β-spodumene. The size of the rutile precipitates is about 0.50 μm and is formed and agglomerated along the grain boundaries. The selected area diffraction pattern of Fig. 8(c), shows the zone axis of [1 $\bar{2}$ $\bar{1}$] of the tetragonal rutile. According to Figs. 7 and 8, the micrographs also reveal in addition the larger precipitates along the grain boundaries, and smaller precipitates as well. During sintering, TiO_2 segregates and agglomerates to form larger precipitates along the grain boundaries and causes the depletion of titanium content in this area. This enhanced segregation is perhaps due to the higher strain field in the regions near the grain boundaries permitting a faster segregation rate.[10]

4. Conclusion

The effects of TiO_2 addition on the morphology and mechanism of sintering of β-spodumene precursor powders have been investigated. The results obtained in the present study were summarized as follows.

1. The crystallinity of the anatase-type TiO_2 was improved with increasing calcining temperature up to 600 °C, and the rutile TiO_2 forms directly as a result of phase transformation of the anatase-type TiO_2. At 700 °C, the phases consist of anatase and rutile TiO_2, and no other phase was identified. The crystallinity of the anatase-type phase decreases, and the rutile phase increases with increaseing calcining temperature from 600 to 700 °C.
2. For the samples of the LAS_4 precursor powders added with 5.0 wt.% TiO_2 and sintered at 950 to 1350 °C for 5 h, the crystallization phases were found to be mostly β-spodumene plus a minor phase of rutile.
3. When LAS_4 is heated at 950 °C for 10 h, a poor sintering, results with the largest voids being

much greater than those sintered at other temperatures. Both fraction and size of pores decrease rapidly with increasing temperature from 950 to 1350 °C. Grain size of the samples sintered at 1350 °C was much greater than that at 1050 °C and was accompanied with discontinuous grain growth.

4. When sintering temperature was raised to 1250 °C, rutile needles were initially precipitated on the surface, and increase in content with sintering temperature.
5. The larger precipitates of TiO_2 about 1.0 μm were mainly segregated and agglomerated at the grain boundaries of β-spodumene crystalline grains. A few precipitates of TiO_2 were dispersed with in β-spodumene crystalline grains.

Acknowledgements

This work was supported by the National Science Council, Taiwan, the Republic of China under Contract No. 81–0405-E-006–09 which is gratefully acknowledged. Help in experimental works and suggestions from Professor M.P. Hung, Professor M.H. Hon, Mr. J.M. Chen and Mr. S.Y. Yau are appreciated.

References

1. Hatch, R. A., Phase equilibrium in the system Li_2O–Al_2O_3–SiO_2. *Am. Mineral.*, 1943, **28**, 471–496.
2. Roy, R. and Osborn, E. F., The system lithium metasilicate–spodumene–silica. *J.Am Chem. Soc.*, 1949, **71**, 2086–2095.
3. Eppler, R. A., Glass formation and recrstallization in the lithium metasilicate region of the system Li_2O–Al_2O_3–SiO_2. *J. Am. Ceram. Soc.*, 1963, **46**, 97–101.
4. Stookey, S. D., Method of Making Ceramics and Product Thereof. US Patent 2,920,971 12 January 1960.
5. Doherty, P. E., Lee, D. W. and Davis, R. S., Direct observation of the crystallization of Li_2O–Al_2O_3–SiO_2 glasses containing TiO_2. *J. Am. Ceram. Soc.*, 1967, **50**, 77–81.
6. Ostertag, W., Fischer, G. R. and Williams, J. P., Thermal expansion of synthetic β-spodumene-silica solid solutions. *J. Am. Ceram. Soc.*, 1968, **51**, 651–654.
7. Nakagawa, K. and Izumitani, T., Metastable phase separation and crystallization of Li_2O–Al_2O_3–SiO_2 glasses, determination of miscibility gap from the lattice parameter of precipitated -quartz solid solution. *J. Non-Cryst. Solids*, 1972, **7**, 168–180.
8. Partridge, G., Nucleation and crystallization in Li_2O–Al_2O_3–SiO_2 glass ceramics. *Glass Technol.*, 1982, **23**, 133–138.
9. Headley, T. J. and Loehman, R. F., Crystallization of a glass-ceramic by euitaxial growth. *J. Am. Ceram. Soc.*, 1984, **67**, 620–625.
10. Hsu, J. Y. and Speyer, R. F., Influences of zirconia and silicon nucleating agents on the devitrification of Li_2O–Al_2O_3–$6SiO_2$ glass. *J. Am. Ceram. Soc.*, 1990, **73**, 3583–3593.
11. Taklcec, E., Senija, D., Dondur, V. and Petranovic, N., Influences of doponts on nucleation and growth of high-quartz solid solution in lithium aluminosilicate glass. *J. Am. Ceram. Soc.*, 1992, **75**, 1958–1963.
12. Rabinovich, E. M., Review: preparation of glass by sintering. *J. Mater. Sci.*, 1985, **20**, 4259–4297.
13. Li, C. T. and Peacor, D. R., The crystal structure of $LiAlSi_2O_6$–II (β-Spodumene). *Z. Krist*, 1968, **126**, 46–65.
14. Knickerbocker, S. H., Kumar, A. H. and Herron, L. W., Cordierite glass-ceramic multiplayer ceramic packaging. *Am. Ceram. Soc. Bull.*, 1993, **72**, 90–95.
15. Knickerbocker, S., Tuzzolo, M. R. and Lawhorne, S., Sinterable β-spodumene glass-ceramics. *J. Am. Ceram. Soc.*, 1989, **72**, 1873–1879.
16. Shyu, J. J. and Wang, C. T., Sintering and properties of $Li_2O{\cdot}Al_2O_3{\cdot}4SiO_2$-borosilicate glass composites. *J. Mater. Res.*, 1996, **11**, 2518–2527.
17. Kobayashi, H., Ishibashi, N., Akiba, T. and Mitamura, T., Preparation of β-spodumene powder by sol-gel process and properties of sintered bodies. *Nippon Seramikkusu Kyokai Gakujutsu Ronbunshi (J. Ceram. Soc. Jpn.)*, 1990, **98**, 703–708.
18. Yang, J. S., Sakka, S., Yoko, T. and Kozuka, H. J., Preparation of lithium aluminosilicate glass-ceramic monolith from metal-alkoxide solution: part 2 Conversion of gel to glass-ceramic monoliths and their properties. *J. Mater. Sci.*, 1991, **26**, 1827–1883.
19. Suzuki, H., Takahashi, J. I. and Saito, H., Low-temperature sintering of fine precursor powders in Li_2O–Al_2O_3–SiO_2 system. *Chem. Soc. Jpn.*, 1991, **10**, 1319–1325.
20. Wen, S. B., Yang, S., Chen, J. M., Wu, N. C. and Wang, M. C., Characterization for synthesis β-spodumene β-spodumene powder by sol-gel process. *J. Ceram. Soc. Jpn.*, 1999, **107**, 1128–1132.
21. Wen, S. B., Wu, N. C., Yang, S. and Wang, M. C., Effect of TiO_2 addition on the crystallization of Li_2O–Al_2O_3–$4SiO_2$ precursor powders by a sol-gel process. *J. Mater. Res, 1999, 3559–3566*.
22. Barry, T. I., Clinton, D., Lay, L. L., Mercer, R. A. and Miller, R. P., The crystallization of glasses based on the eutectic compositions in the system Li_2O–Al_2O_3–SiO_2: part 2 lithium metasilicate-β-eucryptite. *J Mater Sci.*, 1970, **5**, 117–126.
23. Wang, M. C., The effect of TiO_2 addition on the preparation and phase transformation for precursor β-spodumene powders. *J. Mater. Res.*, 1994, **9**, 2290–2297.
24. Wang, M. C., The effect of TiO_2 addition on he thermal behavior for precursor β-spodumene powders during calcinations. *J. Mater. Res.*, 1999, **14**, 97–102.
25. Wang, M. C., Lin, M. H. and Liu, H. S., The effect of TiO_2 addition on the preparation β-spodumene powders by sol-gel process. *J. Mater. Res.*, 1999, **14**, 196–203.